Available online at www.sciencedirect.com
ScienceDirect
International Journal of Machine Tools & Manufacture 47 (2007) 1615–1624
INTERNATIONAL JOURNAL OF MACHINE TOOLS & MANUFACTURE DESIGN, RESEARCH AND APPLICATION
www.elsevier.com/locate/ijmactool

Polishing of polycrystalline diamond by the technique of dynamic friction. Part 2: Material removal mechanism

Y. Chen, L.C. Zhang*, J.A. Arsecularatne

School of Aerospace, Mechanical and Mechatronic Engineering, The University of Sydney, NSW 2006, Australia

Received 23 May 2006; received in revised form 3 November 2006; accepted 6 November 2006
Available online 21 December 2006

Abstract

This paper investigates the material removal mechanisms of PCD using the dynamic friction polishing technique. Scanning electron microscopy, energy dispersive X-ray, X-ray diffraction and Raman spectroscopy were used to identify the mechanisms by analyzing the specimen surfaces and debris produced by polishing. It was found that the material removal occurred in a rather complex way, which can be a chemo-mechanical process, diffusion, oxidization and evaporation, or their combinations.

Keywords: Dynamic friction polishing; Polycrystalline diamond; Material removal mechanism

1. Introduction

As discussed in part 1 of this series research [1], the dynamic friction polishing (DFP) technique utilizes the thermo-chemical reaction induced by the dynamic friction between a diamond specimen and a metal disk rotating at a high peripheral speed (15–25 m/s) and pressure (3–7 MPa) to enable an efficient abrasive-free polishing of single and polycrystalline diamond [2–5]. DFP was developed from a similar technique—thermo-chemical polishing—which heats the whole metal disk to 730–950 °C in a vacuum or H_2 chamber [6–10] to conduct polishing at a much lower velocity (e.g., 2.8 mm/s) and nominal pressure (e.g., 15 kPa). The mechanisms of the thermo-chemical polishing have been described as conversion of diamond into non-diamond carbon by the hot metal with subsequent solution of this carbon in the metal [7,10]. As the polishing progresses, the carbon concentration in the metal plate increases, and the polishing rate decreases. Also, the material removal rate drops with increasing speed of the polishing plate [11], which is attributed to the reduction in the surface contact between the diamond specimen and the plate.

Iwai et al. [3] and Suzuki et al. [4] investigated the material removal mechanism of DFP based on the polishing efficiency in various atmospheres, and carried out X-ray diffraction analyses of the polishing debris and the surface of metal disk tool. They argued that rapid diffusion of carbon from the diamond to the disk and then evaporation of carbon by oxidization were the mechanisms. They ruled out the possibility of carbonization of diamond because they did not find graphite in polishing debris and on the metal disk surface after polishing.

As a matter of fact, owing to the high temperature at the diamond–metal interface, the possibility of conversion of diamond to non-diamond carbon is very high. Furthermore, when grinding or machining ferrous metals with diamond tools, the dominating wear mechanism of diamond is due to its graphitization accelerated by thermally activated catalytic reaction of iron and ambient oxygen [12–14].

The present paper aims to explore whether chemical/phase transformations occur during DFP so that the material removal mechanism can be understood precisely.

2. Experiment

The PCD specimens used were thermally stable diamond compacts, containing 70–75% diamond particles of 25 μm

*Corresponding author. Tel.: +61 293512835; fax: +61 293517060.
E-mail address: zhang@aeromech.usyd.edu.au (L.C. Zhang).

0890-6955/$ - see front matter © 2006 Elsevier Ltd. All rights reserved.
doi:10.1016/j.ijmachtools.2006.11.003

in grain size (the rest are SiC and Si). The diameter and thickness of a typical specimen were 12.7 and 4 mm, respectively. The thermal conductivity of the specimen material was 300 W/mK.

The polishing experiments were conducted on a polishing machine manufactured in-house, as illustrated in Fig. 1. Polishing was conducted by pressing a PCD specimen on to a rotating catalytic metal disk in dry atmosphere. The polishing parameters were: average sliding speed in the range of 15–25 m/s, pressure from 3 to 7 MPa and polishing time from 1 to 5 min. At the end of a test, the polishing debris were collected from around a PCD surface.

The surface roughness was measured using Surftest 402 and Surftest Analyzer (Mitutoyo). Surface topography was observed by an optical microscope (Leica DM RXE). The surface structure and topography were studied using a scanning electron microscope (SEM) Philips 505; at the same time, energy dispersive X-ray (EDX) analysis was used to investigate the chemical compositions.

XRD experiments were performed to study the crystal structure of the PCD specimens and polishing debris. The data were collected on a D5000 Siemens X-ray diffractometer. The diffraction data (peak positions) were analyzed with the aid of the EVA (software) program which permitted a search and match with the JCPDS (Joint Committee on Powder Diffraction Standards) database for the characterization of crystal faces.

Raman spectra were obtained using a Renishaw Raman Microscope (systems 2000) with a CCD array detector. The collection optics was based on a Leica DMLM microscope. The zones for the recording of spectra were selected optically, and were excited by an argon laser (514.5 nm) with 20 mW power directed through the microscope.

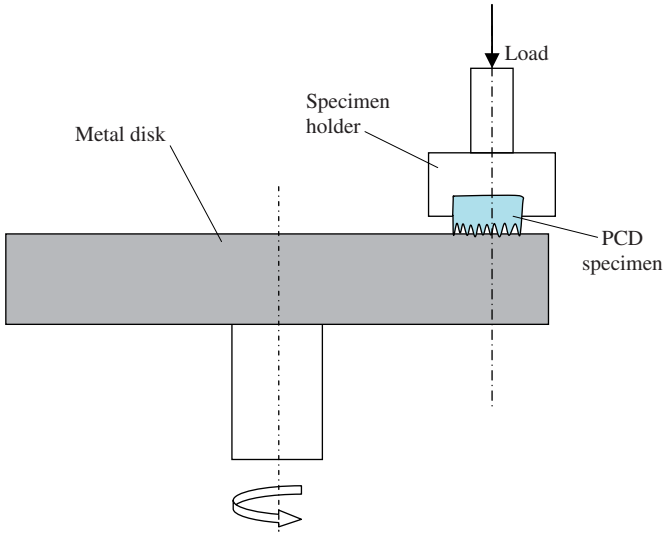

Fig. 1. Schematic illustration of dynamic friction polishing.

3. Results and discussion

3.1. Surface generation

Fig. 2 shows the SEM images of a typical PCD surface. Before polishing, the surface roughness was large (Fig. 2(a)), approximately 1.6 μm Ra. After polishing, a thin metal/oxide film was adhered to the polished PCD surface (Fig. 2(b)) and the surface roughness (Ra) varied with polishing conditions, such as polishing time and disk rotating speed, from 0.1 to 0.6 μm.

After a post-polishing treatment with an acid solution ($HCl + HNO_3$) and/or a mechanical polishing (with SiC paper), the surface roughness of the PCD specimen became much smaller (Ra = 0.2 μm), Fig. 2(c). However, it was not possible to improve the surface roughness any further even with changes in the polishing parameters.

If the PCD surface was further polished by mechanical abrasive polishing with diamond abrasives, the PCD surface roughness could reach Ra = 0.05 μm, as shown in Fig. 2(d).

3.2. Composition and structural analysis

Analyses of the composition and structure of a PCD surface at different stages and the polishing debris can provide information on whether or not a chemical transformation occurs during polishing.

3.2.1. PCD specimen

Fig. 3 shows the components on diamond surfaces at different stages of polishing using EDX analysis in SEM. Before polishing, a large quantity of carbon, some silicon, and little oxygen were detected on the diamond surface (Fig. 3(a)). On the metal/oxides film adhered to the PCD surface, a large quantity of silicon and carbon, and some oxygen and iron were detected together with chromium and nickel (Fig. 3(b)). Once the film was removed, the elements on the clean surface (Fig. 3(c)) became similar to that before polishing (Fig. 3(a)) i.e., a large amount of carbon and silicon, and a small quantity of oxygen and iron.

The structural quality of a PCD surface before and after polishing was assessed using the X-ray diffraction analysis (Fig. 4). Before polishing, diamond and silicon carbide were detected with little coesite (SiO_2) on the surface (Fig. 4(a)). After polishing, maghemite (Fe_2O_3) and awaruite (Ni, Fe) were detected on the metal/oxide film adhered to the surface in addition to the SiC and diamond. After removing the adhered metal/oxide layer, the surface structure was similar to that before polishing. From this XRD analysis, graphite ($2\theta = 30^\circ$) was not detected in any of the above stages, which seems to indicate that there is not any crystalline graphite. However, the possibility of carbonization of diamond still could not be ruled out because amorphous carbon would not give rise to an XRD pattern.

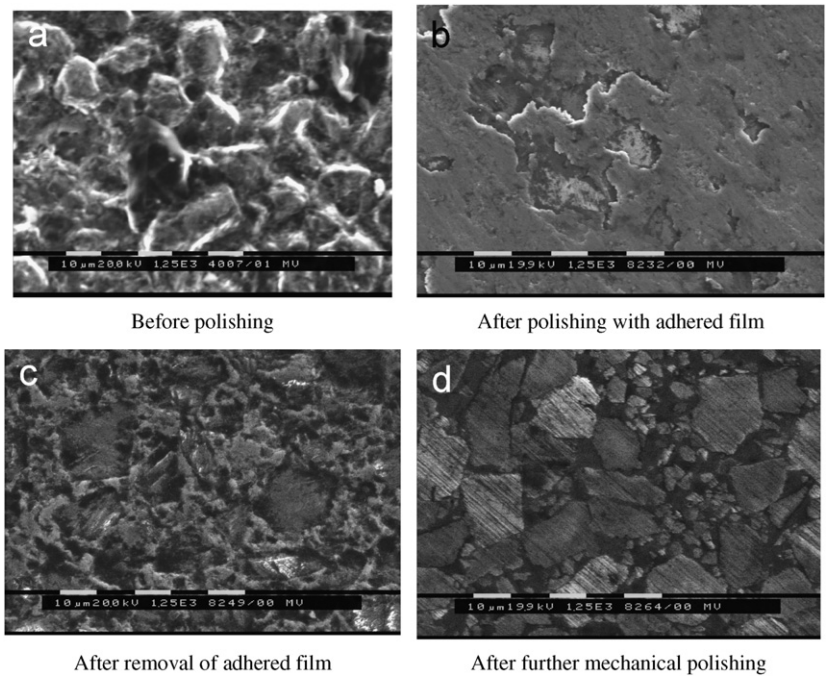

Fig. 2. SEM image of PCD surface before and after polishing: (a) before polishing; (b) after polishing with adhered film; (c) after removal of adhered film; (d) after further mechanical polishing.

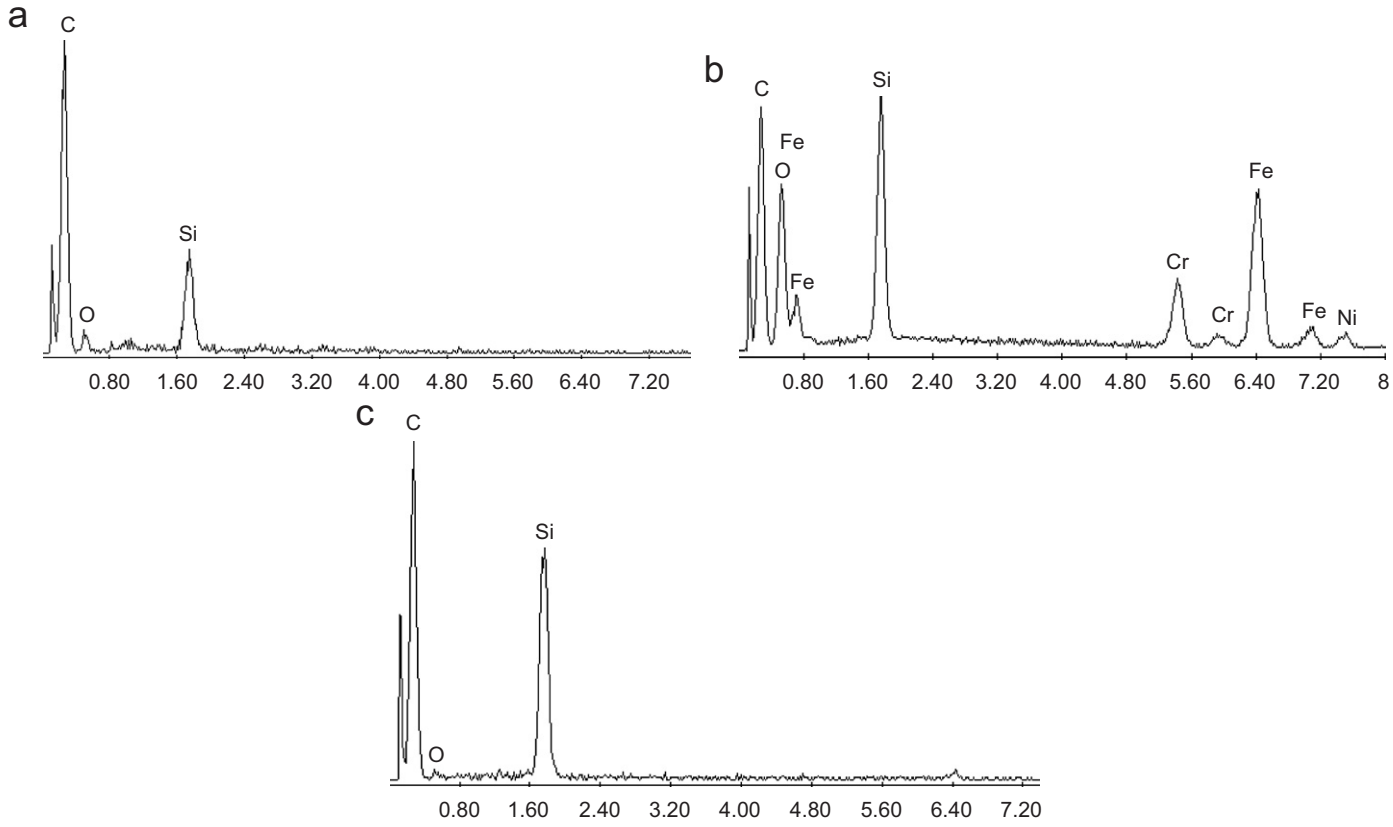

Fig. 3. EDX analysis of PCD surface: (a) before polishing; (b) after polishing: with adhered film; (c) after polishing: cleaned surface.

Raman spectroscopy can be used to distinguish different forms of carbon [15–19]. As shown in Fig. 5(a), the Raman spectrum obtained before polishing presents a sharp intense band at $1334\,cm^{-1}$ which can be assigned to diamond, as the sharp Raman line at $1332\,cm^{-1}$ is the characteristic signature of diamond structure [16,20]. The

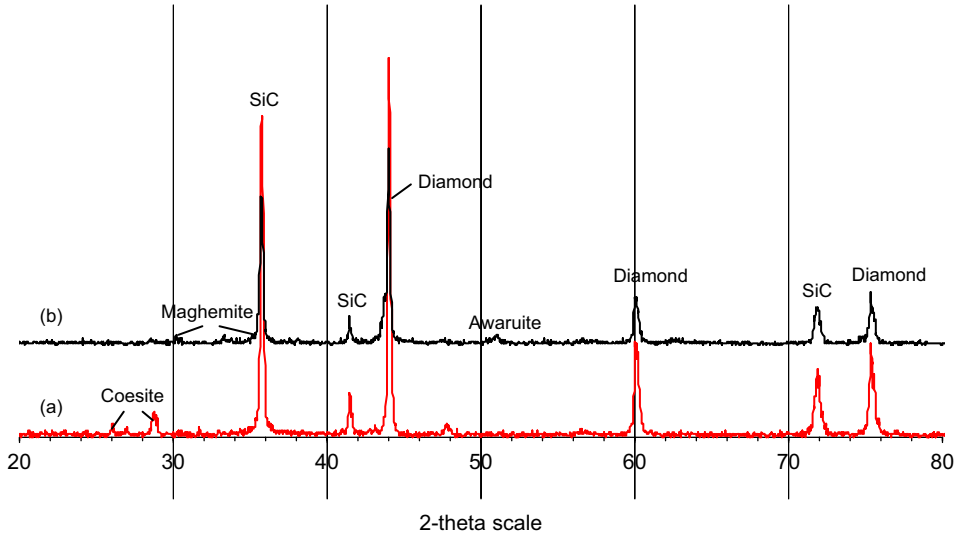

Fig. 4. XRD analysis of PCD surface: (a) before polishing; (b) after polishing with metal/oxide adhered layer.

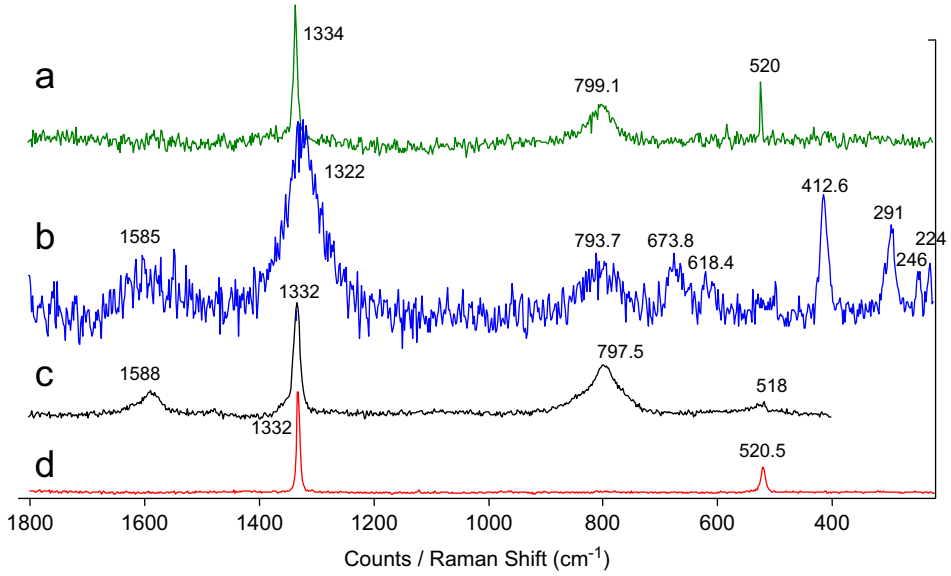

Fig. 5. Raman spectra of PCD specimen surface: (a) before polishing; (b) after polishing with adhered film; (c) after polishing and removal of adhered film; (d) after further polishing with diamond abrasive.

$2\,cm^{-1}$ shift to a higher wave number indicates a compressive residual stress on the PCD specimen, because the Raman band of diamond moves to higher wave number shifts with increasing applied pressure [19]. According to the literature [21,22], the SiC Raman features appear within the 600–1000 and 200–600 cm^{-1} regions. The SiC consists of two main sharp bands at 796 and 973 cm^{-1}. The broad band at 799 cm^{-1} can be assigned to heavily disordered crystalline SiC [23,24], while the band at 520 cm^{-1} results from the contribution of crystalline silicon [25].

For the metal/oxide film adhered to the surface after polishing, the Raman spectrum (Fig. 5(b)) consists of broad bands center at 1322 cm^{-1} (other adhered surface spectra varied 1319–1323 cm^{-1}) and 1585 cm^{-1} (others varied 1585–1597 cm^{-1}). The appearance of these broad bands is attributed to the presence of an amorphous or disordered carbon phase with atoms hybridizing with sp^2 and sp^3 bonds [18,26,27]. The defects composed of sp^3 bonded carbon atoms are revealed in diamond Raman scattering at frequencies $<1332\,cm^{-1}$ [20]. In contrast, the sp^2 (graphitic) bonded species are revealed at $>1332\,cm^{-1}$. The 1322 cm^{-1} band is ascribed tentatively to disordered (defective) sp^3 bonded carbon or lonsdaleite (hexagonal diamond) inclusions [16,20]. The position of the lonsdaleite band maximum could range from 1311 to 1359 cm^{-1} and its width could increase up to 100 cm^{-1}. The movement of the Raman shift towards a low wave number during polishing can be attributed to carbon atoms in sp^3 sites [18], and the Raman peak from diamond (1332 cm^{-1}) moves to

lower wave number shifts and the peak broadens with increasing temperature [19]. If diamond did not change its structure, its Raman spectra would be totally reversible. During the DFP, it seems that some of the cubic diamond has transformed to non-diamond carbon (lonsdaleite or sp^3 carbon) due to its continuous sliding contact with catalytic metals at the friction-induced elevated temperature. When the specimen cools down, this non-diamond carbon still adhered to the surface. Though the band center at 1585–1597 cm^{-1} is hardly detected, the graphite band (around 1580–1606 cm^{-1}) is closely related to the characteristics of disordered sp^2 bonded arrangements, and ascribed to defective or micro-crystalline graphite structures [20,28]. All these indicate the transformation of diamond to non-diamond carbon (disordered or amorphous sp^2 and sp^3) during polishing.

On the spectrum shown in Fig. 5(b), there are also Raman peaks at 224, 246, 291, 413, 618, 674 and 794 cm^{-1}. According to the literature [29–32], the Raman shifts of various forms of iron oxide are obtained in the ranges of 225–227, 243–246, 285–293, 403–415, 498–501, 612–613, 662–665 and 676 cm^{-1}. By comparison with these shifts, the Raman peaks in the metal/oxide film indicate the presence of iron oxides. The 794 cm^{-1} peak might be ascribed to SiC, while an additional peak 618 cm^{-1} attributed to chromium oxide (Cr_2O_3) [30].

After the removal of the adhered metal/oxide layer (Fig. 5 spectrum (c)), Raman peaks at 1588, 1332, 798 and 518 cm^{-1} were detected. These peaks correspond to graphite band (amorphous or disordered sp^2 carbon), crystalline diamond, disordered silicon carbon and silicon, respectively. Compared to the spectrum (a) obtained before polishing, the diamond line relaxed back to that of natural diamond at 1332 cm^{-1} position with a relatively small width. This indicates a non-stressed state of the specimen and a low concentration of structural defects, due to the release of the compressive residual stresses after DFP and the removal of the adhered film. Compared to the spectrum (b) obtained from specimen with the adhered layer, which had a broad lower wave number band at 1322 cm^{-1}, the present 1332 cm^{-1} diamond peak became narrower (spectrum (c)). This indicates that the sp^3 bonded non-diamond carbon has been removed. Additionally, the iron oxides on the adhered film have been removed. However, it was found that the graphite (Raman peak at 1588 cm^{-1}) remained in the specimen and, when the specimen surface was scraped, a thin layer of black carbon could be found. The graphite band (around 1580–1606 cm^{-1}) is stronger in the adhered film removed specimen (spectrum (c)) than that with the adhered film (spectrum (b)). All these indicate that during polishing, transformation of diamond to non-diamond, including graphite (sp^2 bonding) and lonsdaleite (sp^3 bonding), had occurred. It appears that the transformed graphite would be oxidized quickly, and that is why the graphite band was hardly detected on the specimen with an adhered metal/oxide film. But when it is covered by the metal/oxide film, it remained in the specimen. After the film was removed, the intensity of the graphite band became stronger. Oxidation of carbon will be discussed in greater detail in Section 3.3.

After further polishing of the PCD specimen with diamond abrasives, the Raman spectrum (d) in Fig. 5 shows a sharp diamond peak at 1332 cm^{-1} and silicon peak at 520 cm^{-1}. This mechanical polishing process removed graphite, the protruding SiC and possibly a thin layer of diamond that was in contact with metals, and exposed diamond that is free of residual stress. The sharp peak suggests that diamond in the PCD specimen did not deteriorate chemically after DFP (when the diamond did not contact with steel or its temperature did not reach the critical point).

3.2.2. Debris

Through SEM, it was found that the size of the debris varied from a few microns to hundreds of microns. The shapes of the debris were either flake-like or particle-like. EDX revealed that the flake-like debris contained mainly iron, chromium, nickel and oxygen, indicating that they came from the polishing metal disk. Also, these debris were much bigger than the particle-like debris, which could be the result of delamination or chipping from the metal disk during DFP.

A typical particle-like debris, produced during polishing is shown in Fig. 6(a). According to the EDX analysis in Fig. 6(b), it contained carbon, oxygen, silicon, iron, chromium and nickel, which could be from the PCD specimen, the metal disk, and some products of possible reactions.

It was also noted that carbon was always detected with iron, while iron could be detected without carbon. This means that the diamond, removed from the PCD surface, was in contact with iron as products of chemical reaction, while iron could be directly removed by oxidation and/or micro-chipping from the metal disk to form the polishing debris.

According to the XRD analysis of the polishing debris (Fig. 7), they mainly consist of iron oxide Fe_2O_3 (relatively weak intensity) and tridymite SiO_2. There was no indication of crystalline carbon (graphite or diamond), though carbon was detected by the EDX. Carbon might exist in the debris in the forms of non-crystalline or amorphous, since the diffraction signal from these materials is very week.

Fig. 8 shows the Raman spectra of three typical polishing debris. On the low wave number part, bands at 246, 294, 410, 613 and 663 cm^{-1} were observed. According to the literature [29–32], it is reasonable to conclude that iron oxide is the component of the polishing debris. On the high wave number part, broad Raman bands centered at 1319–1321 cm^{-1} were detected. These bands are ascribed tentatively to defective sp^3 bonded carbon or lonsdaleite carbon [16,20]. Additionally, from the X-ray diffraction analysis, only iron oxide and tridymite were detected on the

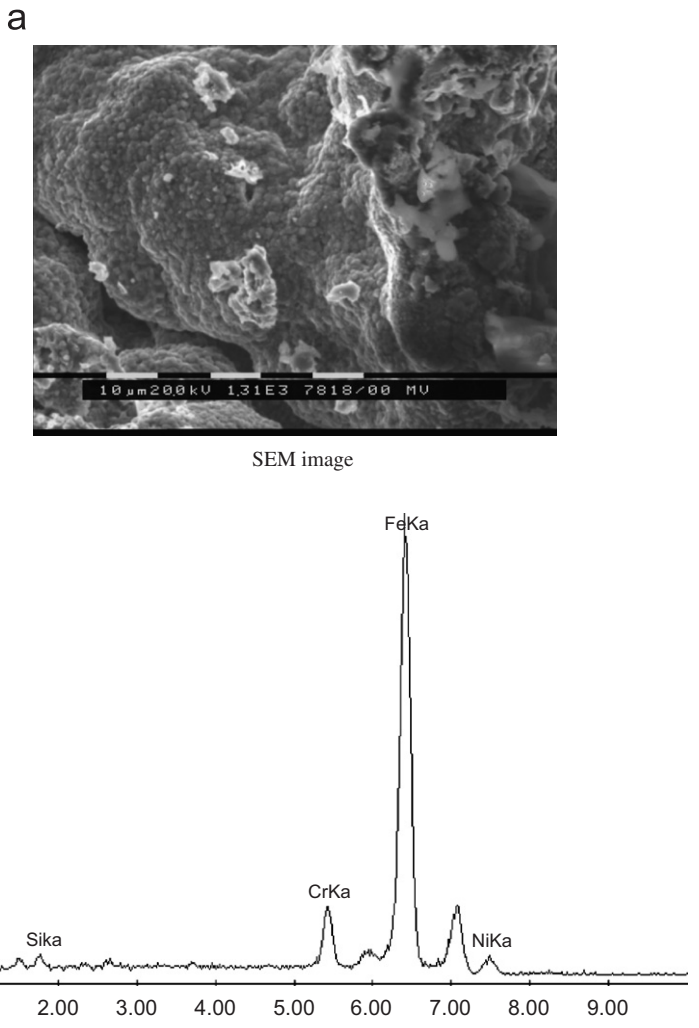

Fig. 6. Particle-like polishing debris: (a) SEM image; (b) EDX analysis.

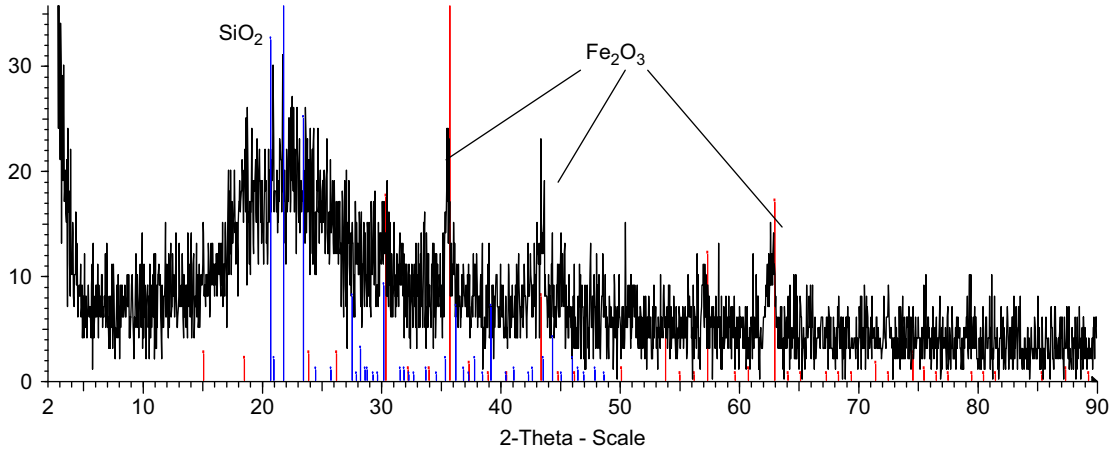

Fig. 7. XRD analysis of polishing debris.

polishing debris, confirming that there was no crystalline carbon in the debris.

It is known that the Raman band position of diamond is a function of temperature [19]. With increasing temperature it moves to lower wave number shifts and its peak broaden. Diamond is stable up to 1300 °C in an inert environment, and up to 600 °C in oxygen environments. Below these temperatures in the corresponding environments, the expected shift to lower wave numbers of diamond is reversible. However, during DFP, the

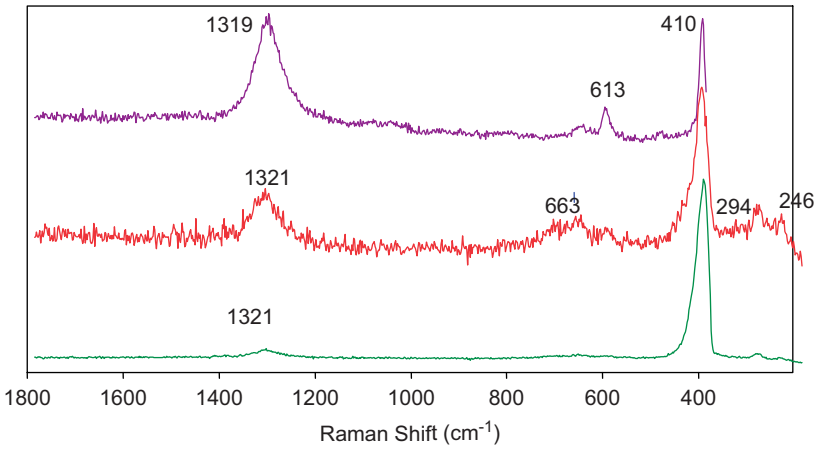

Fig. 8. Raman spectra of typical polishing debris.

diamond in contact with the metal disk appears to lose its diamond structure and transformed to non-diamond carbon (graphite and lonsdaleite), and then was removed mechanically due to the relative PCD specimen-disk sliding. When the debris cooled down, it could not revert to the diamond structure (sharp line at 1332 cm^{-1}).

There was no indication of presence of graphite from this debris. Graphite, which converted from diamond, is likely to oxidize in the oxygen environment and escape as CO/CO_2 gas, or partly remain in the PCD specimen covered by the adhering film.

3.3. Material removal mechanism

In the DFP of PCD, the elevated temperature due to frictional heating converts the diamond on the specimen surface to other forms of carbon, which are then mechanically/chemically removed. The mechanisms involved in material removal are discussed below.

3.3.1. Temperature at the polishing interface

A theoretical model developed to predict the temperature rise in DFP of PCD was presented in part 1 of this series study [1]. Fig. 9 shows the variation of the average interface temperature rise with the sliding speed and applied pressure, which shows the higher values of pressure and sliding speed correspond to a higher heat flux and higher temperature rise. The dependence of temperature rise on sliding speed appears to be linear for a fixed nominal pressure. In the present experiments, the specimens were polished at an average sliding speed in the range of 10–25 m/s and at a pressure from 3 to 7 MPa. From Fig. 9, the estimated temperature rise is over 1000 K. Since the PCD substrate was at room temperature, the actual interface temperature (initial specimen temperature plus temperature rise) is above 1270 K. The high temperature will stimulate the reactions between the polishing metal disk and diamond at the interface.

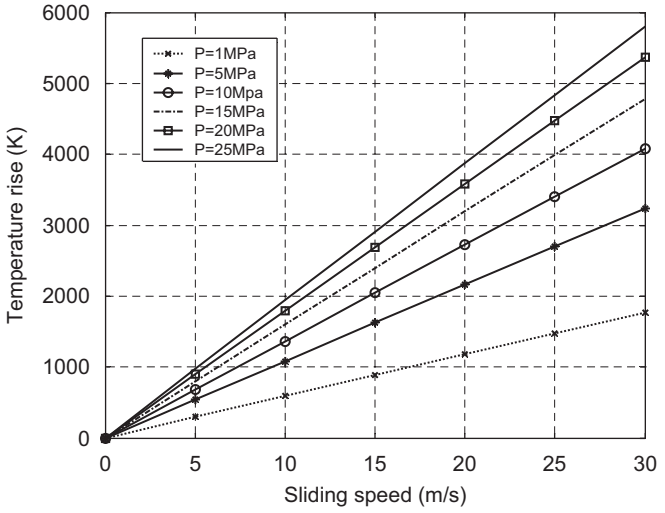

Fig. 9. Variation of average temperature rise with sliding speed at different nominal pressures.

3.3.2. Structural transformation

There are four main types of carbon lattice structures: graphite, amorphous carbon, diamond and lonsdaleite [9]. Thermodynamics indicates that diamond is a metastable phase of carbon, and could convert to graphite at room temperature and atmospheric pressure [33,34]. However, the reaction rate is so slow that the change is normally undetectable. Increased temperature will accelerate its conversion to graphite [35,36]. Generally diamond transforms to graphite at appreciable rates only at high temperatures (>2000 K). However, graphitization occurs at relatively low temperatures (~970 K) when diamond is in contact with transition metals [13,37,38] with intermediate reactivity Fe, Ni, Co, Mn and Cr, which can catalyze the conversion of diamond to graphite at low pressure and at temperatures above 700 °C. The catalytic reaction can be in two directions. An effective catalyst cannot only catalyze the graphite→diamond transition in the stability field of diamond under high pressure, but also the diamond→graphite transition (back

conversion of diamond) in the stability field of graphite at low pressure.

Whilst PCD is being polished by dynamic friction, diamond that is in contact with catalytic metal at temperatures over 1270 K loses its lattice structure and converts into non-diamond carbon. The Raman analyses (Section 3.2) have confirmed the transformation of diamond to non-diamond carbons (sp^2 and sp^3 bonding) had occurred, which is the basic process of the DFP. The non-diamond carbon is then removed mechanically as it was weakly bonded and/or by other chemical reactions.

However, in Iwai et al.'s PCD polishing experiments [3], the adhered films were removed by spraying SiO_2 on the disk and finish polishing at lower pressure on the same machine after their DFP. The transformed non-diamond carbon seemed to have been removed with the adhered film so that no trace of graphite was detected. Also in their XRD analysis, absence of graphite was probably due to the diffraction from non-crystalline graphite (or other carbon forms) was very weak, and the XRD could not detect them. Moreover, according to [39], surface graphitization of diamond is accelerated by oxygen-containing compounds in the gaseous phase. Thin graphite layers are formed on the surface of diamond, and then the graphite not the diamond is oxidized. Hence, during DFP under atmospheric condition, surface graphitization of diamond and its oxidation is to be expected.

3.3.3. Oxidation of carbon

When carbon (including diamond and graphite) is exposed to oxygen bearing environments at elevated temperatures, it would react with oxygen to form CO and/or CO_2 gas. It has been shown that non-diamond carbon oxidizes more rapidly than diamond [40,41]. Also sp^2 bonded carbon is generally known to oxidize faster than sp^3 bonded carbon [41]. The activation energy for graphite varies from 155 to 184 kJ/mol [41,42], while that for a diamond film is from 213 to 240 kJ/mol [40,42,43]. These variations are attributed to differences in the film structure, e.g. morphology, crystallite size, amount of non-diamond carbon, hydrogen, etc. and crystal defects [40]. In oxidizing atmospheres diamond is decomposed at temperatures 700–800 °C via oxidation to gaseous products which are either CO or CO_2 or a mixture of them. At low oxygen pressures, the diamond surface may contain graphite that is also converted to gaseous products at lower activation energy in this temperature regime. According to Alam and Sun's experimental kinetic data [40], at a given oxygen pressure, the oxidation rate increases with increasing temperature. Also at a given temperature, diamond oxidizes faster with increasing oxygen partial pressure.

In the present experiments, PCD is polished under atmospheric conditions, and the temperature at the interface rises above 1270 K; the diamond or transformed non-diamond carbon, exposed to oxygen, would react with oxygen to form CO and/or CO_2 gas. The Raman spectroscopy analysis (Section 3.2) indicates that graphite, which was converted from diamond, had oxidized in the oxygen environment and escaped as CO and/or CO_2 gas, or partly remained in the PCD specimen covered by the adhering film. That is, after the transformation of diamond to non-diamond carbon (sp^2 and sp^3 bonded) has occurred, sp^2 bonded carbon would be oxidized quickly, while sp^3 bonded carbon still remained on the polished metal/oxide adhered surface and polishing debris. Also in Suzuki et al.'s experiments [4], there was a marked increase in the material removal rate in the oxygen atmosphere, supporting oxidation in an oxygen environment.

3.3.4. Diffusion of carbon into the metal disk

Carbon atoms easily diffuse into high carbon soluble metals. These metals include: rare earth alloys and, Fe, Ni and Mo. They have a chemical characteristic known as carbon solubility potential: they are ready to react with any source of free carbon and absorb this carbon into their surface. Such a reaction is easily triggered under the temperature and pressure conditions occurring in the DFP process.

When diamond surface comes into contact with a catalyst metal disk at high temperature, converted carbon atoms in diamond diffuse into the metal disk until the metal is saturated. The diffusion path for atoms from protruding parts of the specimen is shorter and these areas are attacked at a greater rate, and the diffusion rate of graphite is much greater than that of diamond [44]. In Iwai et al.'s [3] EDX analysis, carbon was detected in the polishing metal disk and the adhered film, while Suzuki et al.'s [4] XRD analysis of the disk surface after polishing, a carbonization trace (Fe_3C, cementite) was detected, and EPMA analysis indicated that there was an increase in the carbon element content in the surface in contact with the diamond. These results indicate that there was diffusion of carbon into the metal disk surface. One of the factors involved in diamond polishing is considered to be the diffusion of carbon into the metal disk and form iron austenite after the transformation of diamond to non-diamond carbon.

4. Conclusion

Based on the experimental results and theoretical analyses, the material removal mechanism of dynamic friction polishing can be described as follows: conversion of diamond into non-diamond carbon takes place due to the frictional heating and the interaction of diamond with catalyst metal disk; then a part of the transformed material is detached from the PCD surface as it is weakly bonded; another part of the non-diamond carbon oxidizes and escapes as CO or CO_2 gas and the rest diffuses into the metal disk.

Acknowledgments

The authors wish to thank the Australian Research Council and Ringwood Diamond Material Technologies Pty. Ltd. for their financial support for this research project. The diamond compacts used in the tests were provided by Ringwood DMT Pty Ltd.

References

[1] Y. Chen, L.C. Zhang, J.A. Arsecularatne, C. Montross, Polishing of polycrystalline diamond by the technique of dynamic friction, part 1: prediction of the interface temperature rise, International Journal of Machine Tools and Manufacture 46 (6) (2006) 580–587.

[2] K. Suzuki, N. Yasunaga, Y. Seki, A. Ide, N. Watanabe, T. Uematsu, Dynamic friction polishing of diamond utilizing sliding wear by rotating metal disc, Proceedings of ASPE (1996) 482–485.

[3] M. Iwai, T. Uematsu, K. Suzuki, N. Yasunaga, High efficiency polishing of PCD with rotating metal disc, Proceedings of ISAAT2001 (2001) 231–238.

[4] K. Suzuki, M. Iwai, T. Uematsu, N. Yasunaga, Material removal mechanism in dynamic friction polishing of diamond, Key Engineering Materials 238–239 (2003) 235–240.

[5] M. Iwai, Y. Takashima, K. Suzuki, T. Uematsu, Investigation of polishing condition in dynamic friction polishing method for diamond, in: Seventh International Symposium on Advances in Abrasive Technology, Buras, Turkey, 2004.

[6] M. Yoshikawa, Development and performance of a diamond film polishing apparatus with hot metals, Proceedings of SPIE—The International Society for Optical Engineering 1325 (1990) 210–221.

[7] A.M. Zaitsev, G. Kosaca, B. Richarz, V. Raiko, R. Job, T. Fries, W.R. Fahrner, Thermochemical polishing of CVD diamond films, Diamond and Related Materials 7 (8) (1998) 1108–1117.

[8] H. Tokura, C.-F. Yang, M. Yoshikawa, Study on the polishing of chemically vapour deposited diamond film, Thin Solid Films 212 (1–2) (1992) 49–55.

[9] A.P. Malshe, B.S. Park, W.D. Brown, H.A. Naseem, A review of techniques for polishing and planarizing chemically vapor-deposited (CVD) diamond films and substrates, Diamond and Related Materials 8 (7) (1999) 1198–1213.

[10] J.A. Weima, A.M. Zaitsev, R. Job, G. Kosaca, F. Blum, G. Grabosch, W.R. Fahrner, J. Knopp, Investigation of non-diamond carbon phases and optical centers in thermochemically polished polycrystalline CVD diamond films, Journal of Solid State Electrochemistry 5 (8) (2000) 425–434.

[11] J.A. Weima, W.R. Fahrne, R. Job, Experimental investigation of the parameter dependency of the removal rate of thermochemically polished CVD diamond films, Journal of Solid State Electrochemistry 5 (2) (2001) 112–118.

[12] S. Shimada, H. Tanaka, M. Higuchi, T. Yamaguchi, S. Honda, K. Obata, Thermo-chemical wear mechanism of diamond tool in machining of ferrous metals, CIRP Annals—Manufacturing Technology 53 (1) (2004) 57–60.

[13] N.T. Ikawa, T., Thermal aspects of wear of diamond grain in grinding, Annals CIRP 19(1) (1971) 153–157.

[14] J. Wilks, E. Wilks, Properties and Applications of Diamond, Butterworth-Heinemann, Stoneham, MA, 1994.

[15] K.M. Rutledge, K.K. Gleason, Characterization methods, in: M. Prelas, G. Popovicci, L.K. Bigelow (Eds.), Handbook of Industrial Diamonds and Diamond Films, Marcel Dekker, New York, 1997, pp. 413–480.

[16] D.S. Knight, W.B. White, Characterization of diamond films by Raman spectroscopy, Journal of Materials Research 4 (2) (1988) 385–393.

[17] S.A. Solin, A.K. Ramdas, Raman spectrum of diamond, Physical Review B 1 (4) (1970) 1687–1698.

[18] A.M. Bonnot, Raman microspectroscopy of diamond crystals and thin films prepared by hot-filament-assisted chemical vapor deposition, Physical Review B (Condensed Matter) 41 (9) (1990) 6040–6049.

[19] C. Johnston, A. Crossley, P.R. Chalker, I.M. Buckley-Golder, K. Kobashi, High temperature Raman studies of diamond thin films, Diamond and Related Materials 1 (5–6) (1992) 450–456.

[20] A.M. Zaitsev, Optical properties, in: M.A. Prelas, G. Popovici, L.K. Bigelow (Eds.), Industrial Handbook for Diamond and Diamond Films, Marcel Dekker, New York, 1997.

[21] G. Chollon, R. Naslain, C. Prentice, R. Shatwell, P. May, High temperature properties of SiC and diamond CVD-monofilaments, Journal of the European Ceramic Society 25 (11) (2005) 1929–1942.

[22] S. Karlin, P. Colomban, Micro-Raman study of SiC fibre-oxide matrix reaction, Composites Part B 29B (1998) 41–50.

[23] S. Nakashima, K. Kisoda, H. Niizuma, H. Harima, Raman scattering of disordered SiC, Physica B: Condensed Matter 219–220 (1996) 371–373.

[24] S. Nakashima, H. Harima, Raman investigation of SiC polytypes, Physica Status Solidi (a) 162 (39) (1997) 39–64.

[25] S. Piscanec, A.C. Ferrari, M. Cantoro, S. Hofmann, J.A. Zapien, Y. Lifshitz, S.T. Lee, J. Robertson, Raman spectrum of silicon nanowires, Materials Science and Engineering: C 23 (6–8) (2003) 931–934.

[26] R.O. Dillon, J.A. Woollam, V. Katkanant, Use of Raman scattering to investigate disorder and crystallite formation in as-deposited and annealed carbon films, Physical Review B 29 (1984) 3482–3489.

[27] D. Beeman, J. Silverman, R. Lynds, M.R. Anderson, Modeling studies of amorphous carbon, Physical Review B 30 (1984) 870–875.

[28] J.-K. Yan, L. Chang, Microwave plasma chemical vapor deposition of cone-like structure of diamond/SiC/Si on Si (100), Diamond and Related Materials, Proceedings of the 10th International Conference on New Diamond Science and Technology (ICNDST-10)-ICNDST-10 Special Issue 14(11–12) (2005) 1770–1775.

[29] S. Wang, W. Wang, W. Wang, Z. Jiao, J. Liu, Y. Qian, Characterization and gas-sensing properties of nanocrystalline iron(III) oxide films prepared by ultrasonic spray pyrolysis on silicon, Sensors and Actuators B: Chemical 69 (1–2) (2000) 22–27.

[30] S.C. Tjong, Laser Raman spectroscopic studies of the surface oxides formed on iron chromium alloys at elevated temperatures, Materials Research Bulletin 18 (2) (1983) 157–165.

[31] R.J.H. Clark, M.L. Curri, The identification by Raman microscopy and X-ray diffraction of iron-oxide pigments and of the red pigments found on Italian pottery fragments, Journal of Molecular Structure 440 (1–3) (1998) 105–111.

[32] R.L. Farrow, R.E. Benner, A.S. Nagelberg, P.L. Mattern, Characterization of surface oxides by Raman spectroscopy, Thin Solid Films 73 (2) (1980) 353–358.

[33] F.P. Bundy, W.A. Bassett, M.S. Weathers, R.J. Hemley, H.U. Mao, and A.F. Goncharov, The pressure–temperature phase and transformation diagram for carbon; updated through 1994, Carbon 34(2) (1996) 141–153.

[34] T. Evans, Change produced by high temperature treatment of diamond, in: J.E. Field (Ed.), The Properties of Diamond, Academic Press, London, 1979, pp. 403–424.

[35] V.R. Howes, The graphitization of diamond, Proceedings of the Physical Society 80 (3) (1962) 648–662.

[36] H.T. Hall, The synthesis of diamond, Journal of Chemical Education 38 (1961) 484–489.

[37] C.-M. Sung, M.-F. Tai, Reactivities of transition metals with carbon: implications to the mechanism of diamond synthesis under high pressure, International Journal of Refractory Metals and Hard Materials 15 (4) (1997) 237–256.

[38] Y.V. Butenko, V.L. Kuznetsov, A.L. Chuvilin, V.N. Kolomiichuk, S.V. Stankus, R.A. Khairulin, B. Segall, Kinetics of the graphitization of dispersed diamonds at "low" temperatures, Journal of Applied Physics 88 (7) (2000) 4380–4388.

[39] D.V. Fedoseev, S.P. Vnukov, V.L. Bukhovets, B.A. Anikin, Surface graphitization of diamond at high temperatures, Surface and Coatings Technology 28 (1986) 207–214.
[40] M. Alam, Q. Sun, Kinetics of chemical vapor deposited diamond-oxygen reaction, Journal of Materials Research 8 (11) (1993) 2870–2877.
[41] A. Joshi, R. Nimmagadda, J. Herrington, Oxidation kinetics of diamond, graphite, and chemical vapor deposited diamond films by the thermal gravimetry, Journal of Vacuum Science and Technology A 8 (3) (1990) 2137–2142.
[42] C.E. Johnson, M.A.S. Hasting, W.A. Weimer, Thermogravimetric analysis of the oxidation of CVD diamond films, Journal of Materials Research 5 (11) (1990) 2320–2325.
[43] R.R. Nimmagadda, A. Joshi, W.L. Hsu, Role of microstructure on the oxidation behavior of microwave plasma synthesized diamond and diamond-like carbon films, Journal of Materials Research 5 (11) (1990) 2445–2450.
[44] A.S. Vishnevskii, A.V. Lysenko, T.D. Ositinskaya, V.G. Delevi, Role of diffusion of graphitization in the phase interaction between synthetic diamond and iron, Inorganic Materials 11 (9) (1975).